



OPEN ACCESS

EDITED BY

Aliakbar Hassanpouryouzband,
University of Edinburgh, United Kingdom

REVIEWED BY

Zhenyuan Yin,
Tsinghua University, China
Saeid Ataei Fath Abad,
University of Edinburgh, United Kingdom

*CORRESPONDENCE

Kaixiang Shen,
✉ skxv@163.com
Yingsheng Wang,
✉ gmgs_wys@163.com

RECEIVED 03 November 2023

ACCEPTED 24 January 2024

PUBLISHED 22 February 2024

CITATION

Xu Z, Shen K, Wang Y, Wu J, Liu P, Du J, Huang Q
and Chen C (2024), Consolidation-acidizing
experiments on methane natural gas
sediment skeleton.

Front. Energy Res. 12:1332495.

doi: 10.3389/fenrg.2024.1332495

COPYRIGHT

© 2024 Xu, Shen, Wang, Wu, Liu, Du, Huang and
Chen. This is an open-access article distributed
under the terms of the [Creative Commons
Attribution License \(CC BY\)](#). The use,
distribution or reproduction in other forums is
permitted, provided the original author(s) and
the copyright owner(s) are credited and that the
original publication in this journal is cited, in
accordance with accepted academic practice.
No use, distribution or reproduction is
permitted which does not comply with these
terms.

Consolidation-acidizing experiments on methane natural gas sediment skeleton

Zhenqiang Xu^{1,2}, Kaixiang Shen^{1,2*}, Yingsheng Wang^{1,2*}, Jia Wu³,
Pingli Liu⁴, Juan Du⁴, Qisheng Huang⁴ and Cai Chen⁵

¹Guangzhou Marine Geological Survey, China Geological Survey, Guangzhou, Guangdong, China, ²National Engineering Research Center of Gas Hydrate Exploration and Development, Guangzhou, Guangdong, China, ³Chengdu Synergy Oilfield Technology Service Co. Ltd., Chengdu, Sichuan, China, ⁴State Key Laboratory of Oil and Gas Reservoir Geology and Exploitation, Southwest Petroleum University, Chengdu, Sichuan, China, ⁵Chengdu University of Technology, College of Energy, Chengdu, Sichuan, China

During the development of natural gas hydrates, it is important to ensure the stability of the reservoir. The hydrate reservoirs in the South China Sea are clayey silt sediments, which are prone to sand production and collapse during hydrate dissociation. This study innovatively proposes the idea of consolidation-acidizing for NGH reservoir modification. Based on the core parameters of well A drilling in the Shenhu Sea area of the South China Sea, NGH sediment skeleton samples were artificially prepared. Core sensitivity testing indicates that the NGH reservoir has the potential for acidizing modification. After using tetraethyl orthosilicate to solidify the sample, it was found that Young's modulus of the sample increased by 58.8%, and the compressive strength increased by 54.78%. Although the porosity decreased by 39.33%, the pores were not completely blocked. After the acidizing experiment, the permeability of the consolidated sample was 2.88 mD, and the porosity increased by 10.63%; The permeability of the unconsolidated sample was 1.86 mD, and the porosity decreased by 10.73%. The CT scan images also showed that the pores of the sample after consolidation-acidizing developed uniformly without significant deformation; The unconsolidated sample undergoes severe deformation and sand production after acidizing. This study demonstrates that the consolidation-acidizing modification method is feasible in clayey silt hydrate reservoirs.

KEYWORDS

methane hydrate, hydrate sediment skeleton, consolidation acidizing, sand control, CT scan

1 Introduction

Natural gas hydrate (NGH) is a special ice-like crystalline compound composed of gas molecules and water molecules (Kida et al., 2021). NGH forms under low temperature and high-pressure conditions (Yu et al., 2022). The gases that form hydrates include CH₄, C₂H₆, SO₂, and CO₂, with CH₄ accounting for over 90% (Zhan et al., 2018). NGH has a very high energy density (Zhao et al., 2023a), and the decomposition of 1 m³ methane hydrate produces 164 m³ methane gas. NGH reserves are huge, with almost twice as much hydrocarbon as in proven fossil reserves (Kuang et al., 2019; Yin et al., 2019; Zhang et al., 2020; Ren et al., 2022a; Ma et al., 2022). NGH is considered a promising clean energy source, but due to technological limitations, it has not been commercially developed (Sun

et al., 2021). China has huge methane hydrate reserves, and the South China Sea is an important part of China's NGH exploitation (Chen et al., 2022; Wang et al., 2023a).

The current methods of hydrate reservoir modification include hydraulic fracturing, jet breaking, overlying layer modification, and split grouting (Bai et al., 2023; L et al., 2022; Liu et al., 2020; Ma et al., 2023; Ren et al., 2022b; Du et al., 2023). As the main stimulation method for unconventional oil and gas, hydraulic fracturing is the main modification method for NGH reservoirs. Fracturing can effectively increase the permeability of reservoirs (Too et al., 2018a; Yu et al., 2022). Jet breaking utilizes high-velocity jets to break up NGH sediments, which are then carried to the platform for decomposition. Overlying layer modification involves using CO₂ to form a hydrate above the reservoir, which can stop seawater intrusion during hydrate dissociation. Split grouting is grout injection into the NGH reservoir, where the grout supports the fractures and provides a seepage channel for the gas (Wang et al., 2023b). Almost all NGH modification methods need to promote methane hydrate dissociation (Too et al., 2018b; Cheng et al., 2023), and the solid state of the hydrate will also become a flowing state (Luo et al., 2022). Over 90% of NGH reservoirs are distributed in clayey silt sediments (Ding et al., 2022; Zhang et al., 2022; Wang et al., 2023a; Zhao et al., 2023b; Yang et al., 2023). With the dissociation of hydrates, sand and clay minerals will migrate (Hannun et al., 2022; Li et al., 2022; Sun et al., 2023), causing blockage of seepage channels and even submarine landslides (Sun WT. et al., 2022; Sun HR. et al., 2022; Song et al., 2023), leading to the failure of NGH mining. It is essential to maintain the stability of the NGH reservoir while improving its permeability (Liu et al., 2023).

The authors found that fewer studies have been conducted on acidizing modification of natural gas reservoirs. This paper prepared

a hydrate sediment skeleton based on the mineral composition of NGH in the Shenhu area of the South China Sea. Acidizing experiments were performed on the consolidated sediment skeleton and compared to the unconsolidated sediment skeleton. The experiments verified that the acidizing technology modification is feasible in NGH reservoirs. The research results will provide new insights into the efficient and safe extraction of NGH resources.

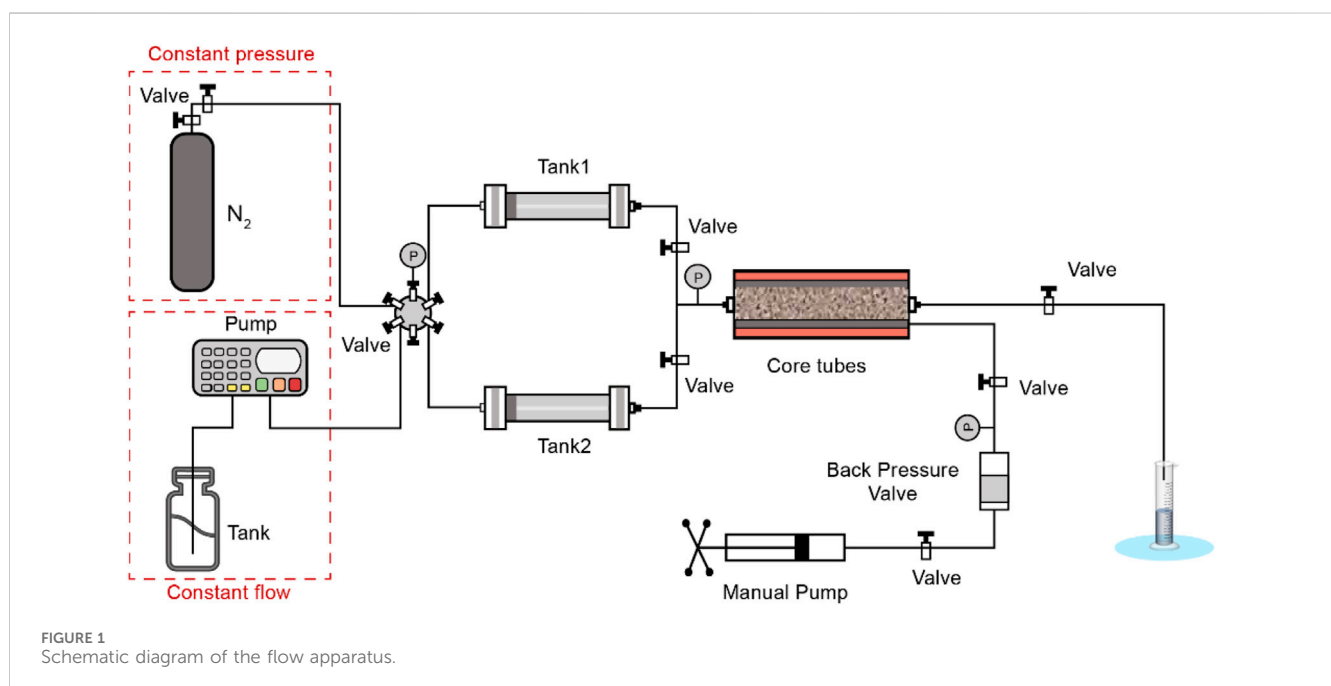
2 Experiment

2.1 Experimental apparatus

The experimental apparatus is shown in Figure 1. The experimental apparatus consists of three structures: a constant-pressure infusion pump, a storage tank, and core tubes. The continuous pressure infusion pump has two modes: constant pressure and constant flow (maximum pressure 30 MPa, maximum flow 20 mL/min), which can provide stable upstream pressure or flow. The storage tank is made of 316 stainless steel with a volume of 500 mL and is used to store displaced acid or consolidation agent. The core tubes hold the sediment skeleton and can provide a confining pressure exceeding 30 MPa.

2.2 Sample preparation

Considering the high cost and limited quantity of hydrate sediment coring, this paper chooses to prepare samples for experiments manually. Experimental samples were prepared by analyzing NGH sediments extracted by the Guangzhou Marine Geological Survey from well A (Figure 2) at Shenhu, Nanhai. The depth of the target NGH reservoir is 266 m, with a porosity of approximately 35.6% and a permeability of approximately 3–20 mD.



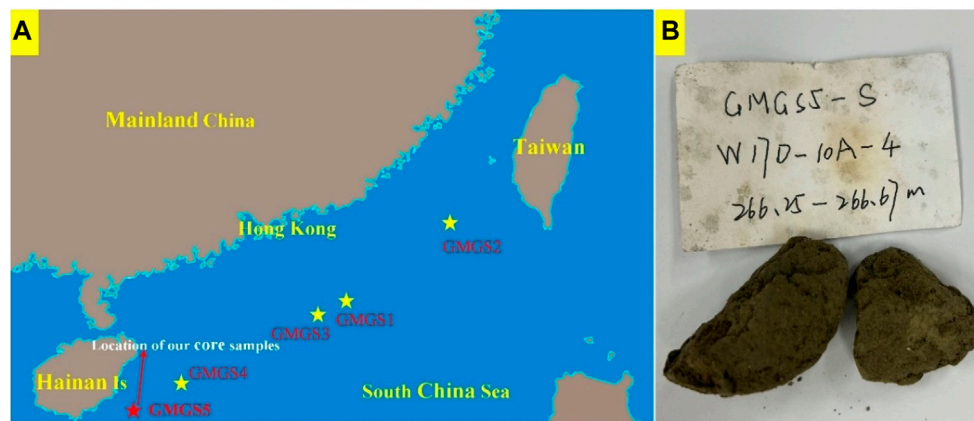


FIGURE 2 NGH sediment sampling location (A); NGH sediment picture (B).

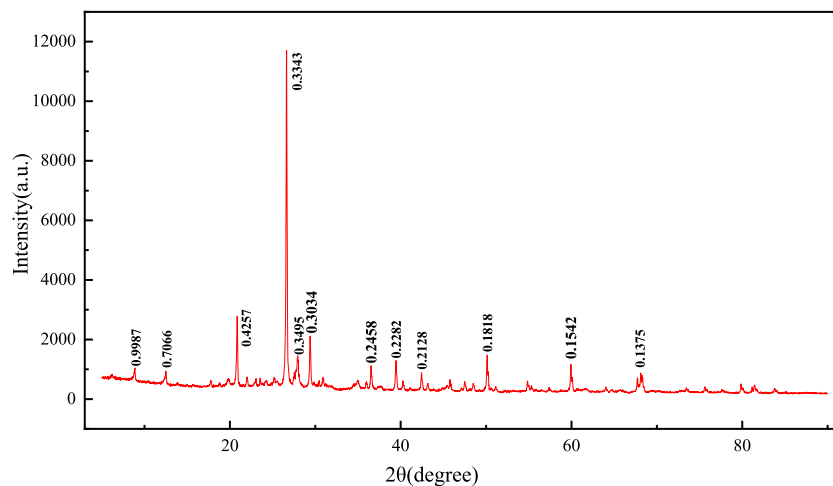


FIGURE 3 XRD image of NGH sediment sample extracted from well.

X-ray diffraction (XRD) (Figure 3) analysis and grain size testing of the extracted sediments, in conjunction with previous studies (Kuang et al., 2019; Chen et al., 2022; Li et al., 2022), determined that the median grain size of the sediments was 8–16 μm and that the minerals were mainly quartz (39%), carbonate (15%), and clay minerals (26%–30%), with the clay minerals being mainly montmorillonite and illite. The mineral content of the target reservoir sediments and the mineral content of the experimental samples are shown in Table 1.

Hydrate Sediment Skeleton Sample Preparation Process: 1) configure the minerals according to the proportions in Table 1; 2) Load the mineral into the mold and compact. In the process of compaction in five times filling, after each filling with the same pressure compaction, before filling with a fine wire to brush the surface rough to prevent delamination and fracture; 3) The pressed cores were sequentially 40°C, 60°C and 70°C water vapor cured and dried; 4) Porosity and permeability testing of artificially prepared

sediment skeleton samples. The specific sediment skeleton preparation process is shown in Figure 4. The prepared sediment skeleton samples with porosity of 30%–40% and permeability of 10–20 mD can meet the experimental requirements.

2.3 Sensitivity experiment

The purpose of NGH reservoir stimulation is to improve permeability and stability. It may cause damage to the reservoir if it is not focused on reservoir protection. The prepared samples were tested for velocity sensitivity, water sensitivity, salt sensitivity, acid sensitivity, alkali sensitivity, and stress sensitivity according to the oil and gas industry standard SY/T5358-2010. Three parallel samples were made for each test to evaluate the sensitivity of the samples and analyze the feasibility of acidizing stimulation in NGH reservoirs.

TABLE 1 Actual mineral content of target reservoir and mineral content of experimental samples.

| Mineral content | Actual Mass proportion | Experimental Mass proportion |
|-------------------|------------------------|------------------------------|
| Quartz/% | 39.0 | 36.4 |
| Calcite/% | 15.0 | 33.7 |
| Kaolinite/% | 5.0 | 4.8 |
| Illite/% | 20.0 | 18.8 |
| Chlorite/% | 5.0 | 3.6 |
| Montmorillonite/% | 1.0 | 2.7 |
| Feldspar/% | 11.0 | 0 |
| Dolomite/% | 3.0 | 0 |
| Others/% | 1 | 0 |

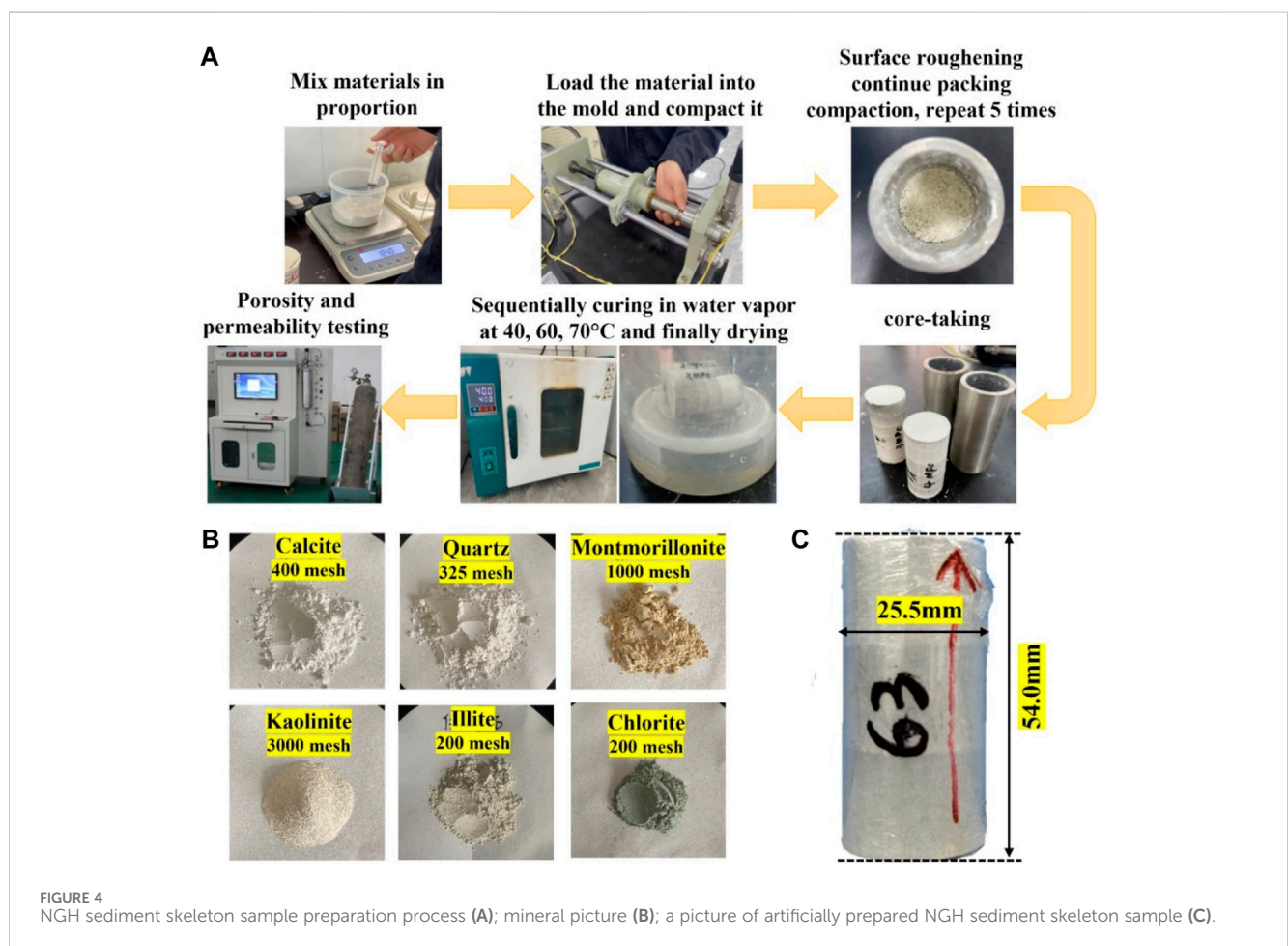


FIGURE 4 NGH sediment skeleton sample preparation process (A); mineral picture (B); a picture of artificially prepared NGH sediment skeleton sample (C).

2.4 Dissolution experiment

Dissolution experiments were used to select the acid solution for acidifying NGH reservoir sediment samples. Prepare rock powder in the proportions in Table 1. The dissolution rates of PORE-A, PORE-A + Perm-A, PORE-A + PORE-B, SA701, solid acid α, solid acid β, and solid acid γ were calculated at 5°C (seafloor temperature). Calculate the dissolution rate of the acid according to the

following formula, make two parallel samples of each acid, and take the average value.

$$\eta = \frac{m_0 + m_1 - m_2}{m_1} \times 100\%$$

Where: η—dissolution rate of minerals, %; m₀—weight of filter paper before reaction, g; m₁—weight of rock powder before reaction, g; m₂—Total weight of filter paper and rock powder after filter drying, g.

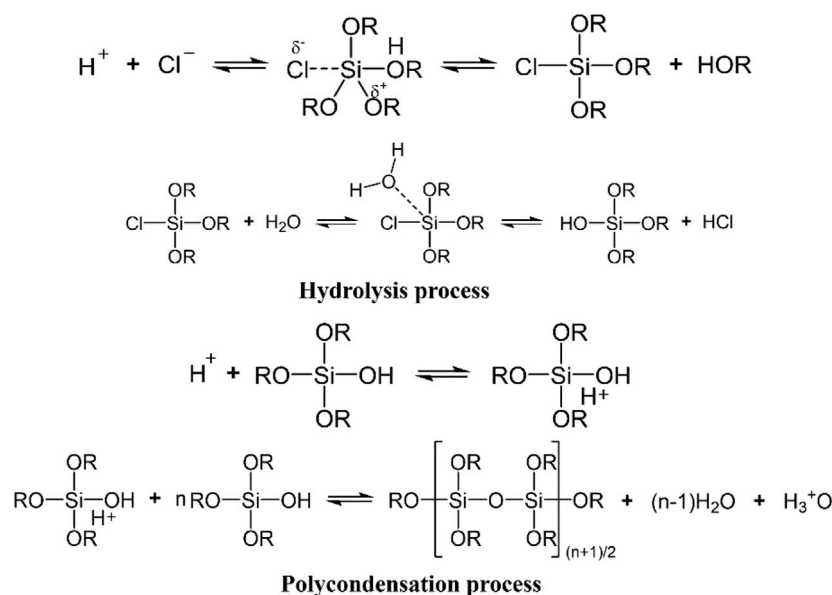


FIGURE 5 Tetraethyl orthosilicate hydrolysis-polycondensation process.

2.5 Optimization experiment of consolidation agent

NGH reservoir sediments are almost weakly consolidated or unconsolidated (Hu et al., 2022), and it is important to ensure reservoir stability during the extraction of NGH. The NGH sediment is mainly composed of fine silt and clay minerals (Tang et al., 2023), and the permeability of the reservoir is low. Tetraethyl orthosilicate (C₈H₂₀O₄Si) is a colorless and transparent liquid at room temperature, with strong fluidity, and does not solidify itself. Hydrolysis catalyzed by acid or alkali generates sol, which is compatible with silicate, so it is easy to form si-o-si solid bonds on the surface of quartz and clay minerals and further condense into a gel. The reaction process is shown in Figure 5. Tetraethyl orthosilicate has low viscosity properties and can form a three-dimensional network structure under the catalysis of acids or bases, making it an ideal NGH sediment skeleton consolidation agent. Conduct experiments to optimize the concentration of tetraethyl orthosilicate. The experimental plan for optimizing the consolidation agent is shown in Table 2.

2.6 Consolidation and acidizing experiments

Weakly consolidated clayey silt NGH sediments are loose and prone to collapse, and acidizing has further weakened the strength of the skeletal consolidation. NGH reservoir sediments in the South China Sea are fine-grained, particles are more easily transported, and acidizing will exacerbate particle transport. Using consolidants to consolidate the NGH sediment skeleton can prevent reservoir sand production and improve stability. Acidizing experiments were performed on the consolidated sediment skeleton and compared to the unconsolidated sediment skeleton.

TABLE 2 Experimental plan for optimizing consolidation agents.

| Catalyzer | Catalyst content (%) |
|--|----------------------|
| 37%HCl,20%HCl,15%HCl | 30%,20%,10 |
| CH ₃ COOH | 30%,20%,10 |
| 15%NH ₃ ·H ₂ O,20%NH ₃ ·H ₂ O,25%NH ₃ ·H ₂ O | 30%,20%,10 |

2.7 Microscopic observation

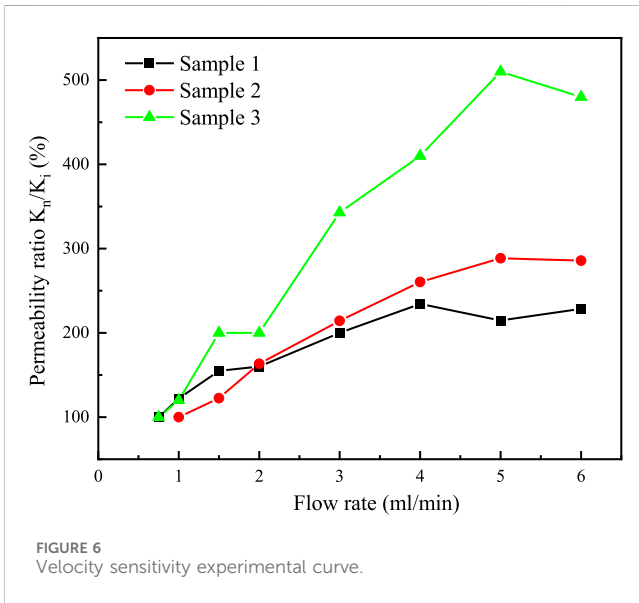
After drying the sample after the experiment, clean the surface with a blower. Scan the sample using a 3D X-ray microanalyzer (Zeiss X-ray Context) produced by Carl Zeiss Microscope GmbH in Germany. With a resolution of 0.95 μm in three dimensions and a high pixel density detector (six megapixels), it can resolve fine details in a complete 3D environment. Heterogeneity in the sample, such as pores, pore size, cracks, porosity, and connectivity, can be characterized and quantified without damaging the sample. The image processing method in this article refers to Ni et al. (Ni et al., 2021).

3 Results and discussion

3.1 Sensitivity experiment

3.1.1 Velocity sensitivity

The velocity sensitive test fluid was 8% standard brine (NaCl: CaCl₂: MgCl₂-6H₂O = 7: 0.6: 0.4). From the test results (Figure 6), it can be seen that the ratio of K_n/K_i increases significantly with increasing flow rate for all three samples (K_n is the original permeability and K_i is the tested permeability), and the critical flow rate ≤ 1 mL/min. According to the industry standard, velocity



sensitivity damage rates are greater than 70%, and the degree of damage is strong. Sediment particles in NGH reservoirs are small, and because they are weakly consolidated, the particles are easily detached and transported with fluid flow. An acid flow rate that is too low in acidizing modification will lead to uneven pore development. Therefore, to ensure the successful implementation

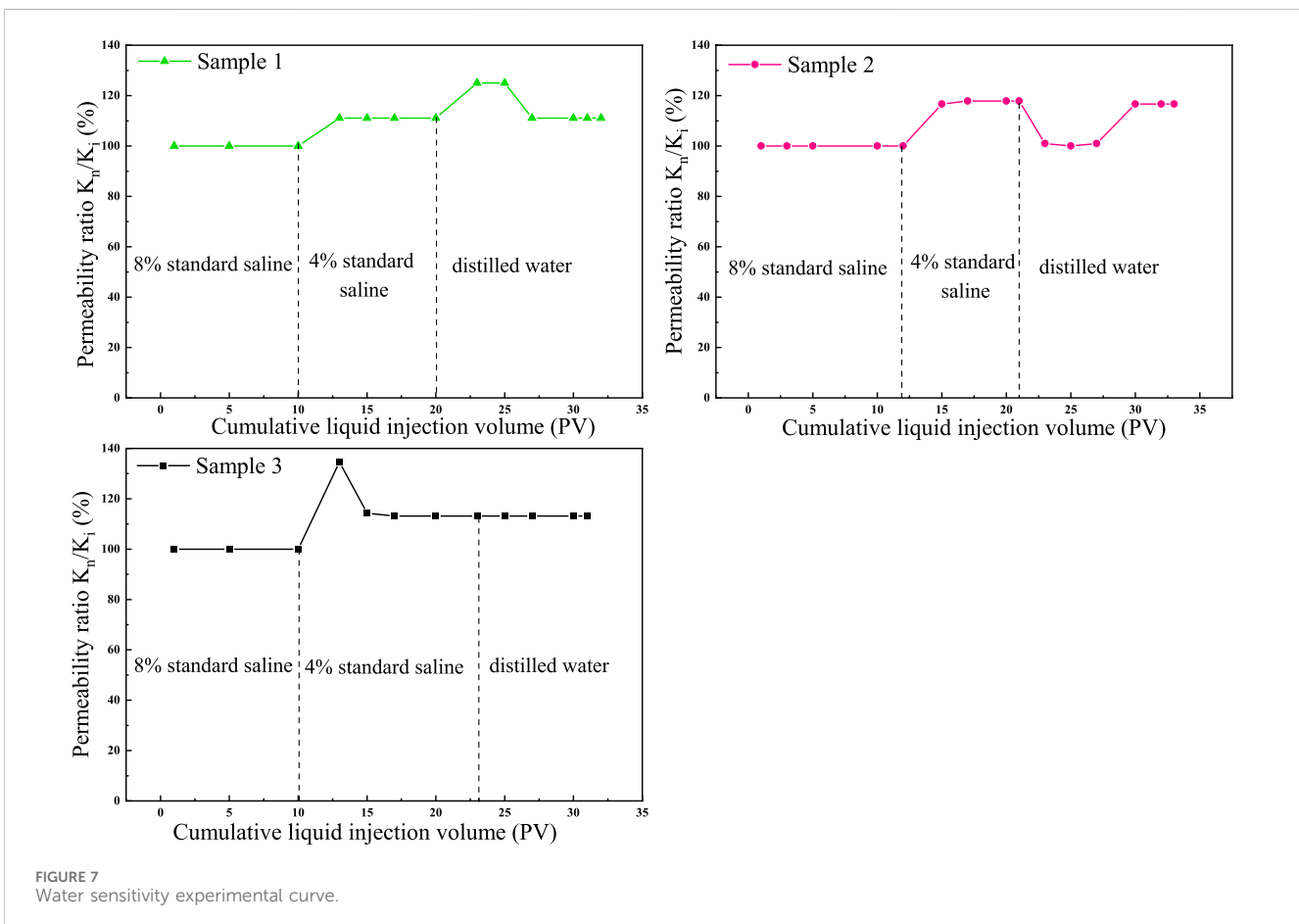
of acidizing modification, the sediment skeleton must be solidified; otherwise, the risk of sand production is exceptionally high.

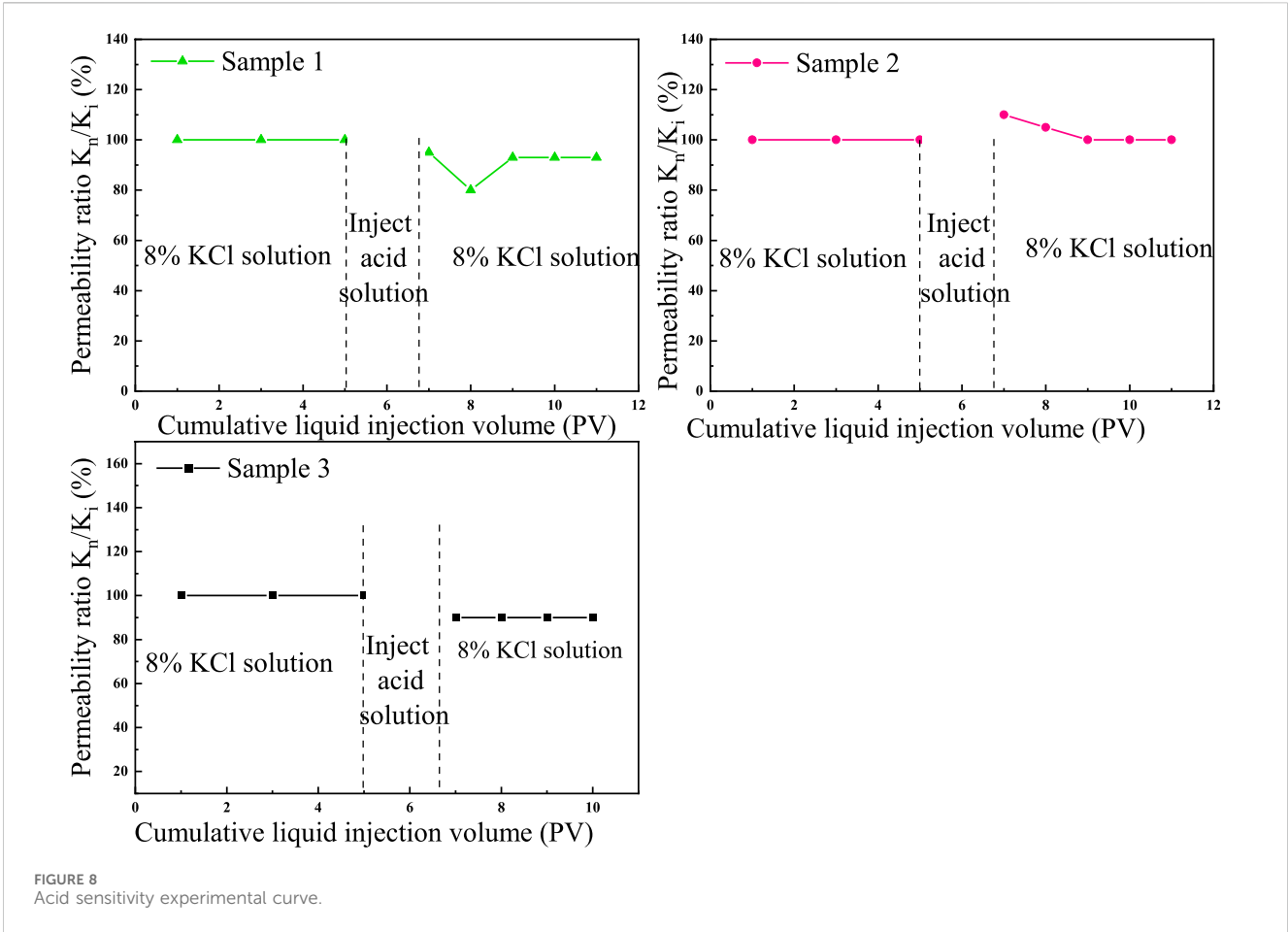
3.1.2 Water sensitivity and salt sensitivity

The NGH sediments in the Shenhu Sea have a high clay mineral content. Clay minerals such as Montmorillonite will expand when encountering low-salinity injection water, and Kaolinite will migrate when encountering low-salinity water, reducing reservoir permeability. The water sensitivity test was conducted using 8% standard brine. The intermediate test fluid was 4% standard saline. The change in permeability ratio during injection is shown in Figure 7. The permeability ratios of the three samples increased slightly with decreasing fluid mineralization. According to the industry standard, water sensitivity damage rates are 5%–30%, which is weak water sensitivity. Montmorillonite is the main water-sensitive mineral, followed by illite and kaolinite. Although the NGH sediments are high in clay minerals, montmorillonite is the least abundant, so the samples are weakly water-sensitive. The damage rate of all three samples in distilled water is less than 20%, and there is no need to conduct salinity reduction sensitivity experiments.

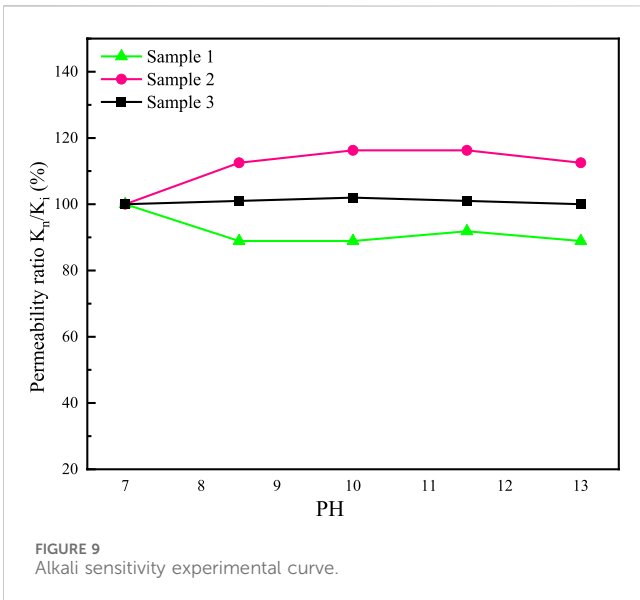
3.1.3 Acid sensitivity

The acid sensitivity experiment reflects the acid's effect on the reservoir's permeability. Hydroxide precipitates, fluoride precipitates, fluorosilicates, and gels produced by the acid and reservoir minerals may block the pores. Acidizing disrupts the reservoir's original





shown in Figure 8. Samples 1 and 3 showed increased permeability after acidizing, indicating an improvement in sample porosity. Sample 2 showed no significant change in permeability after acidizing, probably because dislodged particles blocked some of the pores. According to industry standards, acid sensitivity damage rates are less than 5%, and NGH reservoirs can be acid stimulated.



3.1.4 Alkali sensitivity

The alkali sensitivity test fluid was 8% KCl solution, and the KOH solution changed its pH. The permeability ratio is shown in Figure 9. Sample 2 had a slight decrease in permeability during the pH increase, sample 1 had a slight increase in permeability, and sample 3 had no significant change in permeability. According to industry standards, Sample 2 has an alkali sensitivity damage rate of 5%–30%, which is a weak alkali sensitivity. Sample 1 and 3 have an alkali sensitivity damage rate of less than 5%, which is no alkali sensitivity damage.

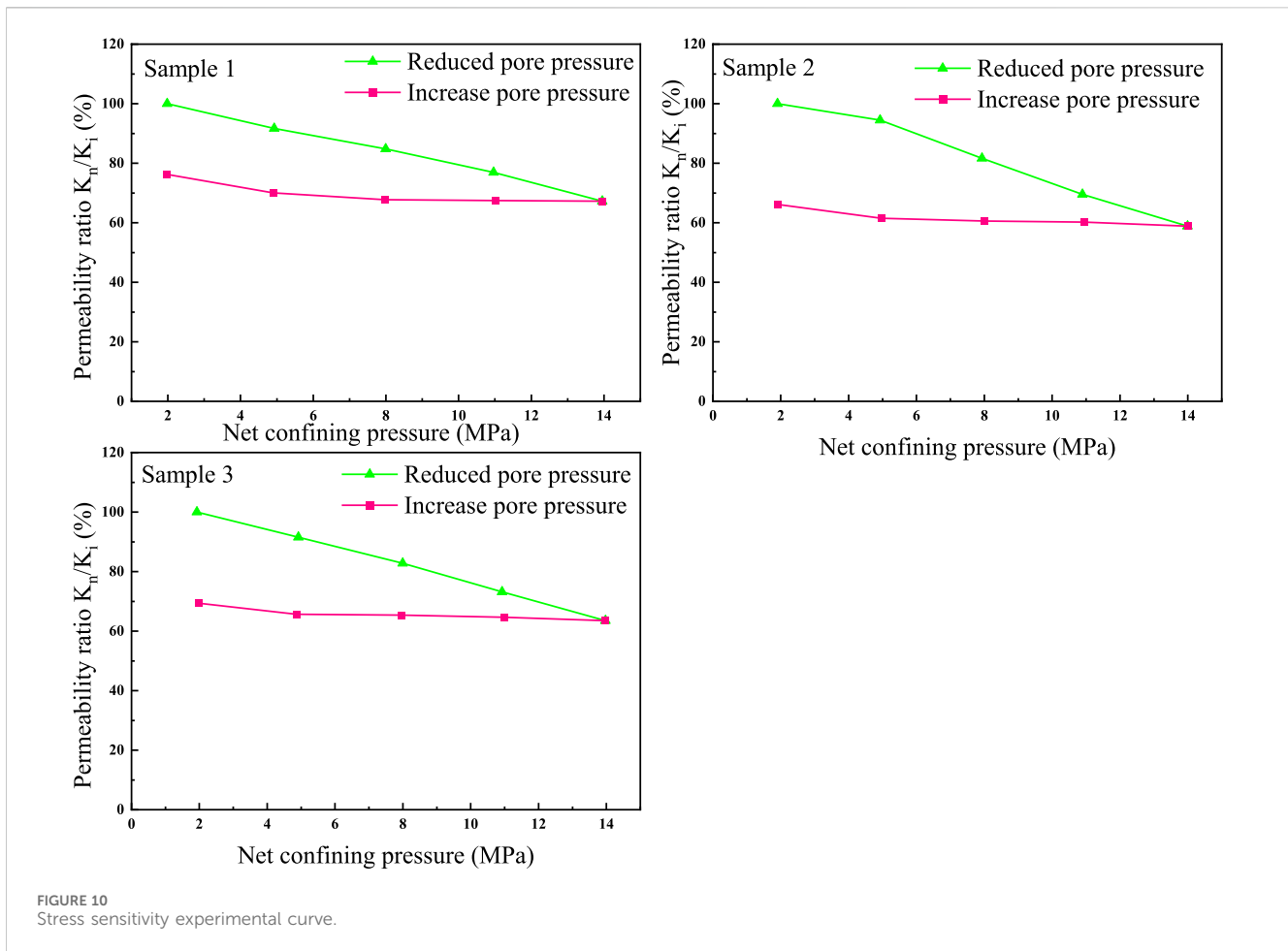
3.1.5 Stress sensitivity

With the internal fluid output, reservoir pore pressure reduction will change the reservoir’s original force balance, leading to changes in the pore structure and affecting the fluid flow in the reservoir. Stress sensitivity factors include reservoir lithology, cementation strength, pore structure, particle sorting, and pore pressure change rules.

The use of back-pressure variations brings it closer to the reality of the NGH reservoir. Refer to the GMGS3-W19 station model Wan

structure, aggravating velocity sensitivity, and the released clay particles swell and transport, leading to decreased permeability.

Permeability was measured before and after acidizing using an 8% KCl solution. The acid solution for the sensitivity test was 12% PORE-A + 3% Perm-A. The permeability ratio change curve is



(Wan et al., 2018) et al. developed during hydrate depression mining. The water depth of 1,273.9 m is converted to a top pressure of 12.86 MPa, and the *in-situ* stress gradient is 0.02597 MPa/m, which calculates the overburden pressure to be approximately 16.3 MPa. The initial pressure at the bottom boundary of the hydrate layer was 14.3 MPa, and the net overburden pressure was calculated to be 2 MPa, which was used as the initial net stress value of the sample. Considering the low bottomhole pressure in the late production period, the minimum bottomhole pressure was set to 2.3 MPa. The confining pressure was used to replace the overburden pressure. The initial backpressure value was 14.3 MPa, which was varied sequentially to 11.3, 8.3, 5.3, and 2.3 MPa, and then slowly increased to 14.3 MPa, all with a net stress interval of 3 MPa.

The stress sensitivity curve is shown in Figure 10. The critical stress of all three samples was 8 MPa, the stress-sensitive damage rate was around 30%–40%, and the irreversible permeability damage rate was around 30%, with moderate stress sensitivity.

3.2 Dissolution experiment

The average dissolution rate of each acid solution at 5°C is shown in Figure 11. PORE-A can dissolve through carbonate rocks, and the dissolution results of Perm-A and PORE-B systems are similar, and the dissolution rates are all in the range of 15%–35%. SA, solid acid γ, and

solid acid β acid systems are prone to precipitation at high concentrations. Three acid systems, 8% PORE-A + 1% Perm-A, 5% PORE-A + 5% PORE-B, and 10% solid acid α, were selected for the experiments.

3.3 Optimization experiment of consolidation agent

Tetraethyl orthosilicate solidified well under HCL catalysis, formed precipitates, and did not solidify after 24 h under CH₃COOH and NH₃·H₂O catalysis (Figure 12). When tetraethyl orthosilicate:37% HCl is 7:3, it loses fluidity to form frozen gel-like crystals within 9 min, and the mechanical strength after curing is low. C₈H₂₀O₄Si:20%HCl = 9:1 has a gelling time of more than 2 h, good fluidity, completes solidification at 6 h, and solidifies to form glassy crystals with high mechanical strength. The C₈H₂₀O₄Si:20%HCl = 9:1 formulation was used for the consolidation experiments as it was characterized by low-temperature consolidation, long gelling time, and good fluidity.

3.4 Consolidation and acidizing experiments

3.4.1 Properties before and after consolidation

Inject the consolidation agent into the sample at a displacement of 0.5 mL/min and evaluate the changes in permeability, porosity,

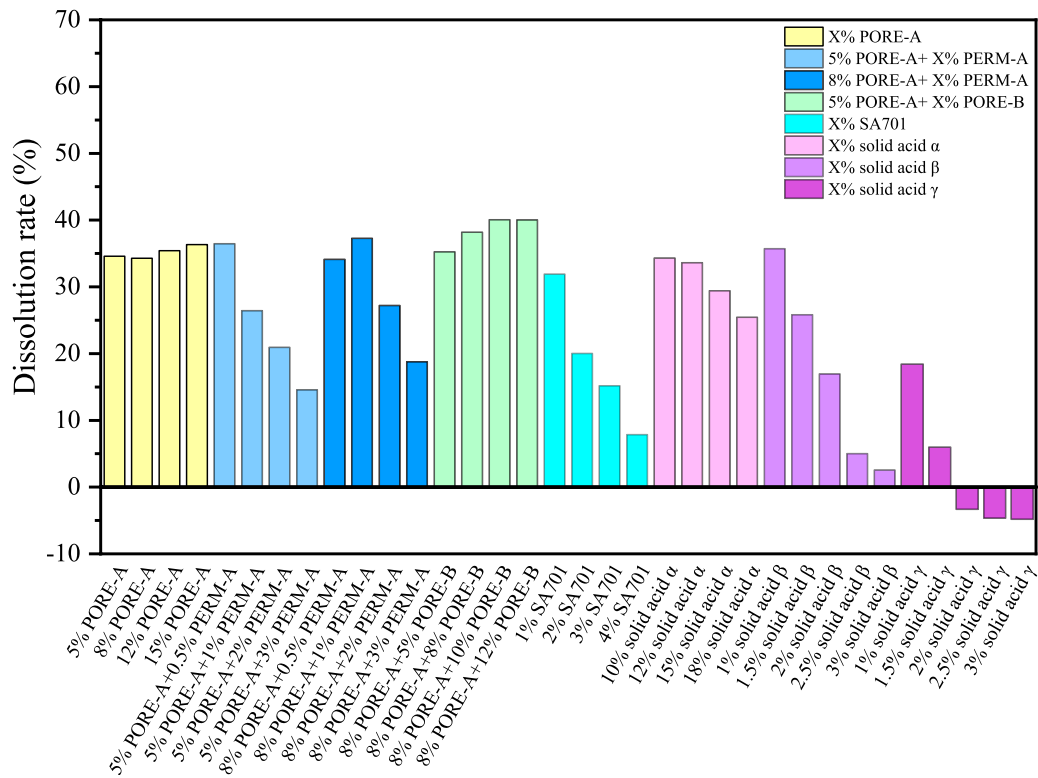


FIGURE 11 The average dissolution rate of different acids at 5°C.

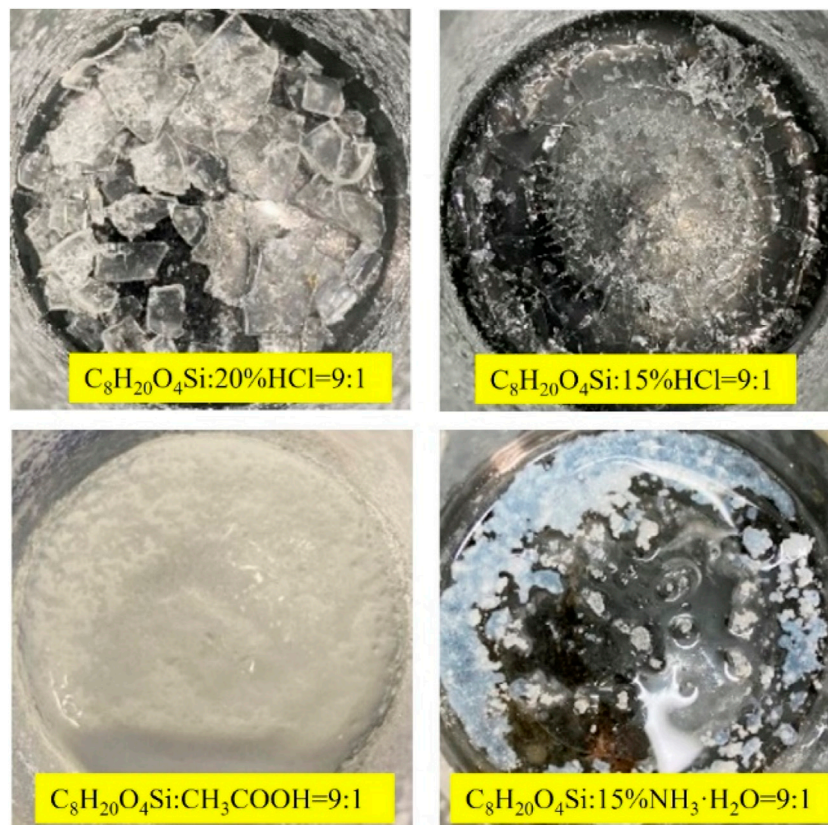
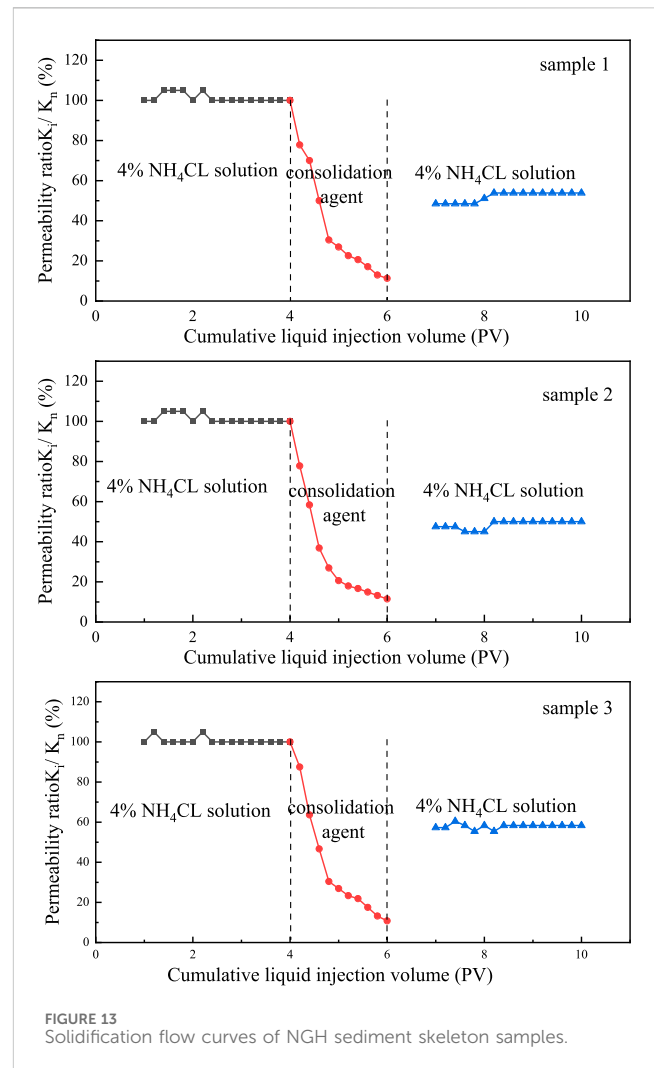


FIGURE 12 Picture of acid/base catalyzed $C_8H_{20}O_4Si$ consolidation.

TABLE 3 Physical properties of NGH sediment skeleton before and after consolidation.

| NO. | Pre-consolidation permeability (mD) | Post-consolidation permeability (mD) | Pre-consolidation porosity (%) | Post-consolidation porosity (%) | Young's modulus after consolidation (MPa) | Poisson's ratio after consolidation | Compressive strength after consolidation (MPa) |
|-----|-------------------------------------|--------------------------------------|--------------------------------|---------------------------------|---|-------------------------------------|--|
| 1 | 2.44 | 1.07 | 38.92 | 22.67 | 255.72 | 0.25 | 2.3 |
| 2 | 2.24 | 0.97 | 37.56 | 23.36 | 276.83 | 0.27 | 2.6 |
| 3 | 2.36 | 1.03 | 37.87 | 23.22 | 153.74 | 0.20 | 2.4 |



compressive strength, and pore throat structure after 6 h of consolidation. The experimental results are shown in Table 3.

The increase in fluid viscosity during consolidation agent injection leads to a rise in drive pressure. During the infusion of the consolidation agent, the permeability decrease was significant, and the driving pressure increased up to 7.8 MPa (Figure 13: K_n is the original permeability, and K_i is the tested permeability). The consolidation agent occupies some of the pore space, resulting in a decrease in the porosity of the samples (Figure 14). The retention of permeability of the consolidated samples was around 56%, and the retention of porosity was 38%–41%. From the CT scanning results (Figure 15B), it can be clearly seen that the pore diameter of the sample after consolidation is obviously reduced, the pore distribution is more uniform, and the pore distribution in the exit section of the sample is denser compared with that in the middle section and the entrance section, which is similar to that before consolidation, indicating that the system of the consolidation agent has been uniformly infused into the sample. It can be seen from the slice map that the “small black dots” of the sample before consolidation are denser, and the “big black dots” are occasionally seen. After solidification, the sample is more dense, the distribution of “small black dots” is more sparse, and the pore size of “large black

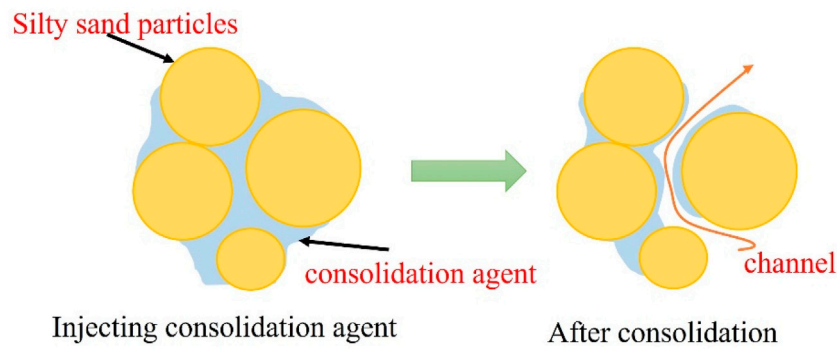


FIGURE 14 Schematic diagram of the consolidation process of the NGH sediment skeleton.

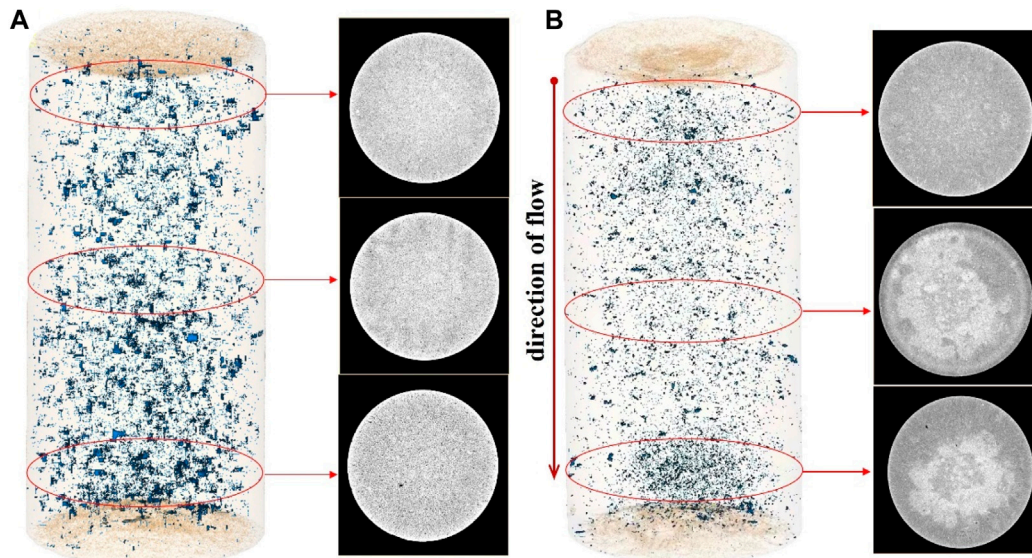


FIGURE 15 CT scans of NGH sediment skeleton samples before (A) and after consolidation (B). (Note: the blue portion indicates pore development and the light yellow portion indicates the sample matrix).

dots” is obviously smaller. As seen from the 3D and slice map, the pores of the consolidated samples were not completely blocked but retained some porosity and connectivity.

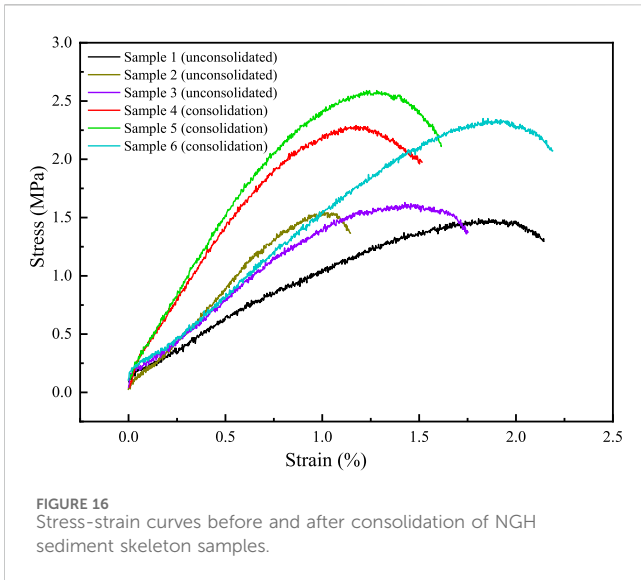
As shown in Figure 16, the mechanical properties of the consolidated sample are improved. The average compressive strength of the unconsolidated samples was 1.57 MPa, the average Young’s modulus was 144.05 MPa, and the average Poisson’s ratio was 0.27. The average compressive strength of the consolidated samples was 2.43 MPa, the average Young’s modulus was 228.76 MPa, and the average Poisson’s ratio was 0.24. After consolidation, the compressive strength and Young’s modulus of the sample increase, and Poisson’s ratio decreases, indicating that the resistance to deformation of the sample increases.

3.4.2 Acidizing experiment

The samples were subjected to acidizing experiments using three acid solutions: 8% PORE-A + 1% Perm-A, 5% PORE-A + 5% PORE-

B, and 10% solid acid α . The results of the experiment are shown in Table 4.

The results of the 8% PORE-A + 1% Perm-A acid solution experiments showed that: The skeleton of the unconsolidated sample was severely deformed, and serious sand production occurred during the experiment. From the CT scan (Figure 17A), it can be seen that the skeleton at the injection end of the unconsolidated sample is difficult to maintain and undergoes severe deformation, and there is a clear interface in the middle part of the sample, suggesting that the silt transported to this place blocked the pore throat channel, resulting in the pore space not being developed at the outflow end of the core. It indicates that there is a problem with sand and gravel transport in the unconsolidated sample. In contrast, the skeleton of the consolidated sample (Figure 17B) was only slightly deformed, the acid reacted uniformly with the minerals in the flow direction, and no sand production occurred during the experiment, indicating that the



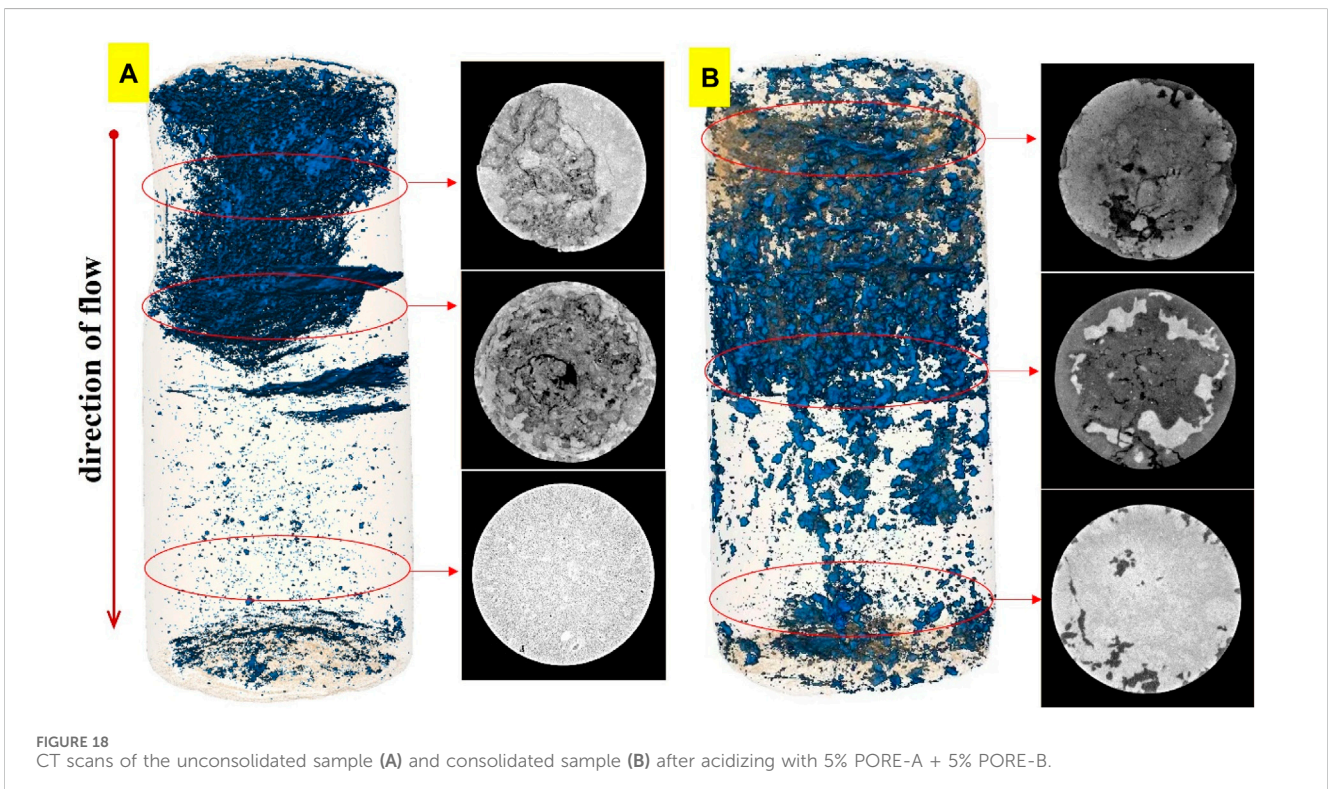
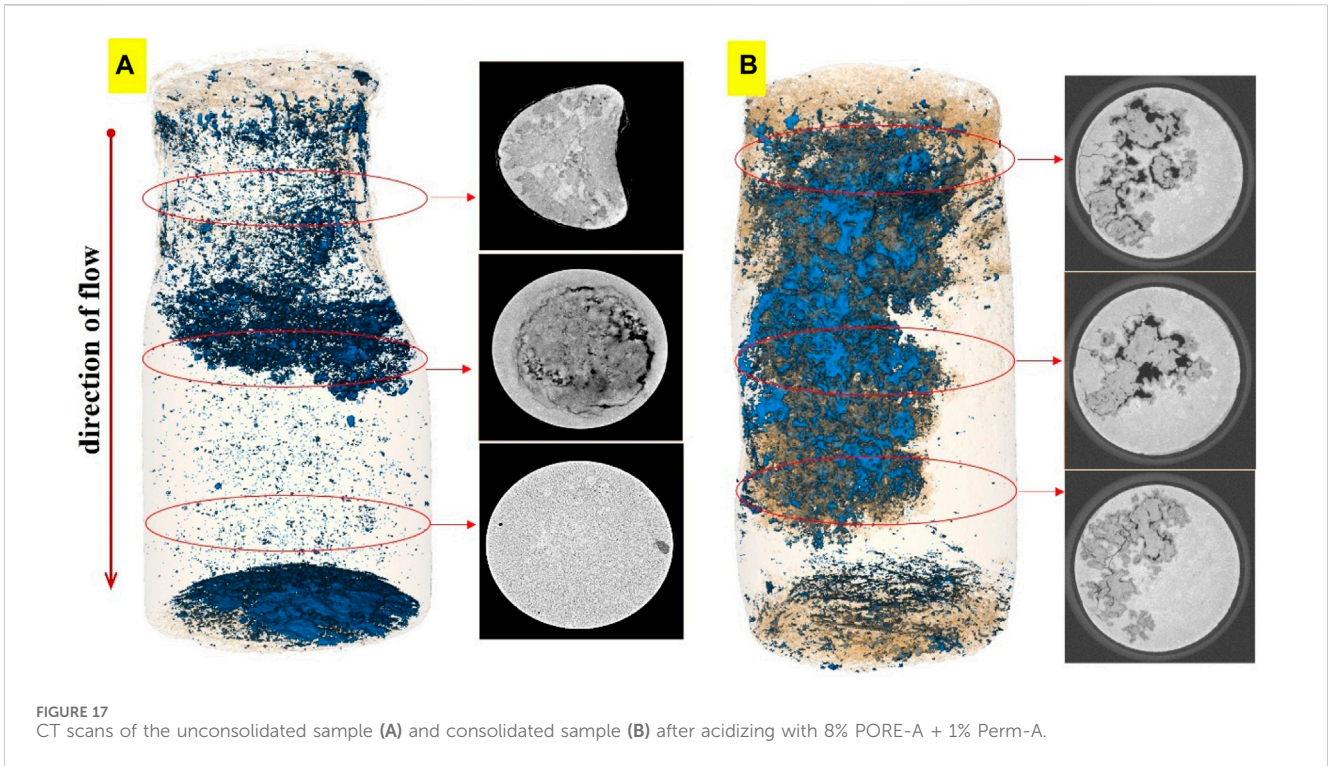
consolidation agent can effectively prevent sand production and improve the stability of the sediment skeleton. The acidizing of the consolidated samples increased the permeability by 120.97% and porosity by 82.94%.

Similarly, the 5% PORE-A + 5% PORE-B and 10% solid acid α experiments showed that the solidified samples had better stability and were less prone to sand production. Figure 18 shows similar results to Figure 17. In Figure 18A, it can be clearly seen that the pore space at the injection end of the unconsolidated sample is very well developed. Still, the pore space at the outflow end is not clearly developed. There is a clear interface in the middle part of the sample, which suggests that the skeleton produces a serious amount of sand, and that the sand and gravel transportation blocks the seepage passage. Figure 18B shows the CT scan of the consolidated sample after acidizing, the result shows that the pore development of the consolidated sample is uniform, and the sample does not show sanding and deformation problems. Figure 19 shows the results of the 10% solid acid α flow experiment. Because of the slower reaction rate of solid acid α , the unconsolidated samples (Figure 19A) did not show significant pore throat plugging, but less pore development was observed in the unconsolidated samples compared to the consolidated samples (Figure 19B), which suggests that minor sanding may have occurred in the unconsolidated samples. The compressive strength test results also show that the consolidated samples have better compressive strength.

Unlike conventional reservoirs, NGH reservoirs are highly heterogeneous in terms of sediment distribution and hydrate saturation (Ren et al., 2022a; Ren et al., 2022b), which complicates consolidation-acidizing modification of NGH reservoirs. In the South China Sea, NGH sediments are predominantly clayey-silty sediments, and the presence of natural gas in the reservoir is in the form of cements at contracts, grain coating and pore-filling. The hydrate pore-filling type has the strongest cementing effect on the sand and gravel. With the further dissociation of gas hydrate, the sand and gravel cannot be effectively supported, which causes changes in the reservoir structure, and may cause sand production or collapse. Preventing reservoir sand production

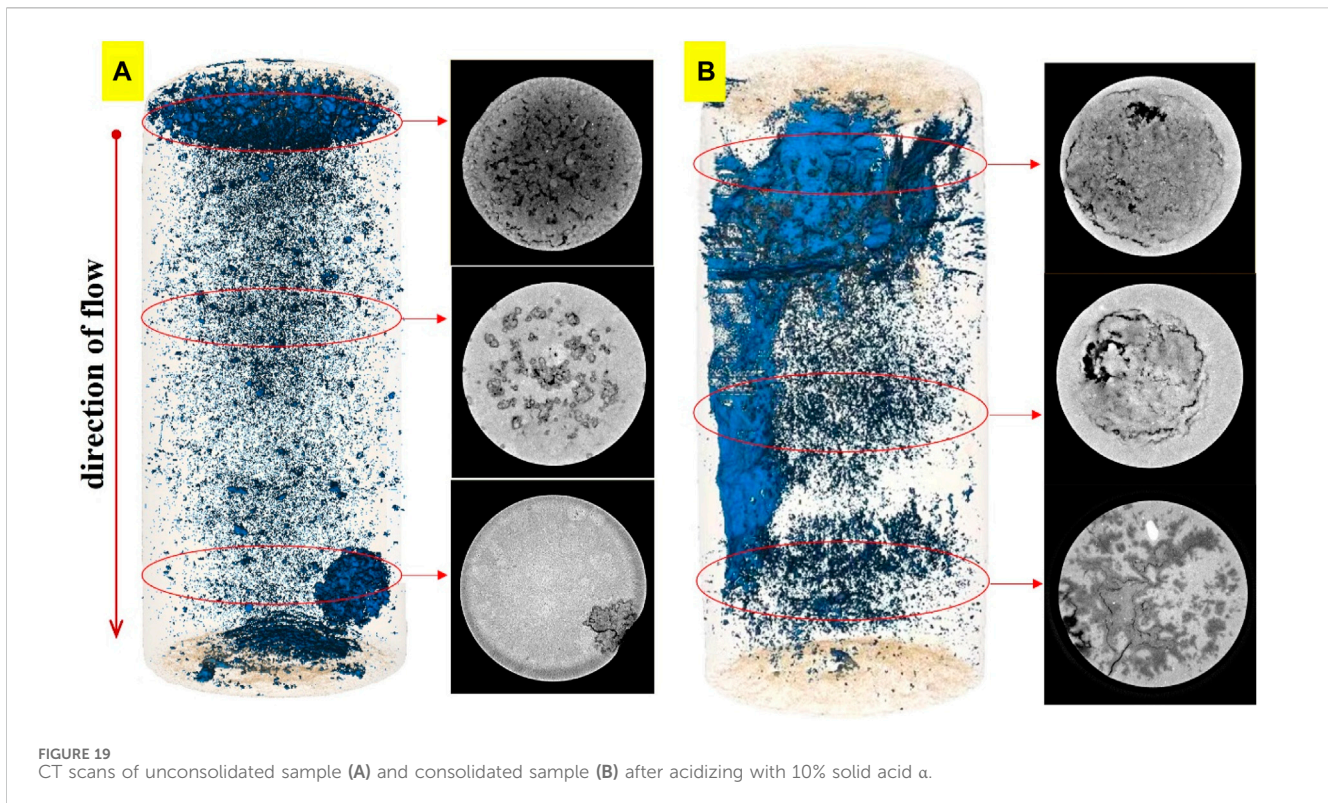
TABLE 4 Physical properties of sediment skeleton samples before and after acidizing.

| Acid | Consolidation or not | Permeability before acidizing (mD) | Permeability after acidizing (mD) | Porosity before acidizing (%) | Porosity after acidizing (%) | Compressive strength (MPa) | Skeleton deformation | Sand production |
|------------------------|----------------------|------------------------------------|-----------------------------------|-------------------------------|------------------------------|----------------------------|----------------------|-----------------|
| 8% PORE-A + 1% Perm-A | No | 2.59 | 1.37 | 37.83 | 20.34 | - | serious | serious |
| | Yes | 1.24 | 2.74 | 23.33 | 42.68 | 1.1 | slight | No |
| 5% PORE-A + 5% PORE-B | No | 2.21 | 1.42 | 36.77 | 29.65 | 0.6 | moderate | moderate |
| | Yes | 1.12 | 2.52 | 23.05 | 40.63 | 1.3 | No | No |
| 10%solid acid α | No | 2.39 | 1.86 | 38.42 | 33.53 | 0.8 | No | moderate |
| | Yes | 1.17 | 2.88 | 23.11 | 42.30 | 1.0 | No | No |



and maintaining reservoir stability are important aspects of developing NGH reservoirs. In this paper, we take the mud silt type weakly cemented NGH reservoir as the research object, and innovatively propose the consolidation-acidizing method of NGH reservoir modification. The experimental results show

that the consolidant can effectively improve the strength and stability of the sediment skeleton, maintain the skeleton morphology during the hydrate dissociation process, and inhibit the sand production of the reservoir. Compared with the unconsolidated samples, the consolidated samples were



stable in acid modification, not easy to produce sand, and had uniform pore development after acidification. It shows that consolidation-acidizing modification is feasible in natural gas reservoirs.

4 Conclusion

The clayey silt NGH reservoir sediments were used to solidify the reservoir skeleton samples using tetraethyl orthosilicate, and then the samples were subjected to acidizing experiments using the acid solution and compared with the unconsolidated samples. The pore development morphology of the samples was observed by CT scanning, and the feasibility of the consolidation-acidizing modification method was verified. The main research findings are as follows:

- 1) The Young's modulus of the samples after consolidation with tetraethyl orthosilicate increased by 58.8% and the compressive strength increased by 54.78%. Although the porosity of the samples decreased by 39.33%, the consolidation agent did not completely block the pores.
- 2) The permeability of the consolidated-acidizing sample was 2.88 mD with a 10.63% increase in porosity, while the permeability of the acidizing unconsolidated sample was 1.86 mD with a 10.73% decrease in porosity. The consolidation agent can effectively improve the stability of the NGH sedimentary skeleton and prevent sand production or collapse of the reservoir. The condition of acidizing and reforming exists in the consolidated sediment skeleton. And the acidizing sediment skeleton has good pore development.

- 3) The CT scan images show that the unconsolidated sediment samples have severe deformation of the skeleton after acidizing and there is sand production. In contrast, the consolidated sediment samples have no obvious skeleton deformation after acidizing, the pore development is uniform, and no sand production is found.

Data availability statement

The raw data supporting the conclusion of this article will be made available by the authors, without undue reservation.

Author contributions

ZX: Writing–review and editing. KS: Writing–original draft, Data curation, Formal Analysis, Project administration, Supervision, Writing–review and editing. YW: Data curation, Formal Analysis, Project administration, Supervision, Writing–original draft, Writing–review and editing. JW: Writing–original draft. PL: Conceptualization, Data curation, Formal Analysis, Methodology, Resources, Software, Supervision, Validation, Writing–original draft, Writing–review and editing. JD: Conceptualization, Data curation, Formal Analysis, Methodology, Resources, Software, Supervision, Validation, Writing–original draft, Writing–review and editing. QH: Data curation, Investigation, Methodology, Writing–original draft, Writing–review and editing. CC: Data curation, Formal Analysis, Funding acquisition, Writing–review and editing.

Funding

The author(s) declare that no financial support was received for the research, authorship, and/or publication of this article. This research was funded by Marine Economy Development Foundation of Guangdong Province (GDNRC [2022] 44) and the Guangdong Major Project of Basic and Applied Basic Research (NO.2020 B0301030003).

Conflict of interest

Author JW was employed by Chengdu Synergy Oilfield Technology Service Co Ltd Chengdu.

References

- Bai, Y. J., Clarke, M. A., Hou, J., Liu, Y. G., Lu, N., Zhao, E. M., et al. (2023). Study on improved efficiency of induced fracture in gas hydrate reservoir depressurization development. *Energy* 278, 127853. doi:10.1016/j.energy.2023.127853
- Chen, H., Du, H., Shi, B., Shan, W. C., and Hou, J. Q. (2022). Mechanical properties and strength criterion of clayey sand reservoirs during natural gas hydrate extraction. *Energy* 242, 122526. doi:10.1016/j.energy.2021.122526
- Cheng, F. B., Wu, Z. R., Sun, X., Shen, S., Wu, P., Liu, W. G., et al. (2023). Compression-induced dynamic change in effective permeability of hydrate-bearing sediments during hydrate dissociation by depressurization. *Energy* 264, 126137. doi:10.1016/j.energy.2022.126137
- Ding, J. P., Cheng, Y. F., and Yan, C. L. (2022). Research on sand control effect and micro-plugging mechanism of sand control medium in the development of natural gas hydrate reservoir. *J. Petroleum Sci. Eng.* 215, 110703. doi:10.1016/j.petrol.2022.110703
- Du, J., Huang, Q., Liu, P., Fu, Y., Lan, X., Chen, X., et al. (2023). Advances in nanocomposite organic coatings for hydraulic fracturing proppants. *Gas Sci. Eng.* 118, 205103. doi:10.1016/j.jgsce.2023.205103
- Hannun, J. A., Al-Raoush, R. I., Jarrar, Z. A., Alshibli, K. A., and Jung, J. W. (2022). Fines effect on gas flow in sandy sediments using CT and pore networks. *J. Nat. Gas Sci. Eng.* 108, 104834. doi:10.1016/j.jngse.2022.104834
- Hu, C., Jia, Y. G., and Duan, Z. B. (2022). Pore scale study of the permeability anisotropy of sands containing grain-coating and pore-filling hydrates. *J. Petroleum Sci. Eng.* 215, 110590. doi:10.1016/j.petrol.2022.110590
- Kida, M., Yoneda, J., Masui, A., Konno, Y., Jin, Y., and Nagao, J. (2021). Mechanical properties of polycrystalline tetrahydrofuran hydrates as analogs for massive natural gas hydrates. *J. Nat. Gas Sci. Eng.* 96, 104284. doi:10.1016/j.jngse.2021.104284
- Kuang, Y. M., Yang, L., Li, Q. P., Lv, X., Li, Y. P., Yu, B., et al. (2019). Physical characteristic analysis of unconsolidated sediments containing gas hydrate recovered from the Shenhu Area of the South China sea. *J. Petroleum Sci. Eng.* 181, 106173. doi:10.1016/j.petrol.2019.06.037
- Li, X. Y., Hu, H. Q., Wang, Y., and Li, X. S. (2022). Experimental study of gas-liquid-sand production behaviors during gas hydrates dissociation with sand control screen. *Energy* 254, 124414. doi:10.1016/j.energy.2022.124414
- Liu, T., Wu, P., You, Z. S., Yu, T., Song, Q., Song, Y. X., et al. (2023). Deformation characteristics on anisotropic consolidated methane hydrate clayey-silty sediments of the South China Sea under heat injection. *Energy* 280, 128190. doi:10.1016/j.energy.2023.128190
- Liu, X. Q., Sun, Y., Guo, T. K., Rabiei, M., Qu, Z. Q., and Hou, J. (2022). Numerical simulations of hydraulic fracturing in methane hydrate reservoirs based on the coupled thermo-hydrologic-mechanical-damage (THMD) model. *Energy* 238, 122054. doi:10.1016/j.energy.2021.122054
- Liu, X. Q., Zhang, W. D., Qu, Z. Q., Guo, T. K., Sun, Y., Rabiei, M., et al. (2020). Feasibility evaluation of hydraulic fracturing in hydrate-bearing sediments based on analytic hierarchy process-entropy method (AHP-EM). *J. Nat. Gas Sci. Eng.* 81, 103434. doi:10.1016/j.jngse.2020.103434
- Luo, T. T., Zou, D., Zhao, X. D., Zhang, C. Y., Han, T., and Song, Y. C. (2022). Strength behaviours of methane hydrate-bearing marine sediments in the South China Sea. *J. Nat. Gas Sci. Eng.* 100, 104476. doi:10.1016/j.jngse.2022.104476
- Ma, K. L., Li, D. L., and Liang, D. Q. (2023). Reservoir stimulation Technologies for natural gas hydrate: research progress, challenges, and perspectives. *Energy and Fuels* 37 (14), 10112–10133. doi:10.1021/acs.energyfuels.3c01464
- Ma, X. L., Jiang, D. D., Lu, J., Fang, X. Y., Yang, P., and Xia, D. Q. (2022). Hydrate formation and dissociation characteristics in clayey silt sediment. *J. Nat. Gas Sci. Eng.* 100, 104475. doi:10.1016/j.jngse.2022.104475
- Ni, H., Liu, J., Huang, B., Pu, H., Meng, Q., Wang, Y., et al. (2021). Quantitative analysis of pore structure and permeability characteristics of sandstone using SEM and CT images. *J. Nat. Gas Sci. Eng.* 88, 103861. doi:10.1016/j.jngse.2021.103861
- Ren, J. J., Liu, X. H., Niu, M. Y., and Yin, Z. Y. (2022a). Effect of sodium montmorillonite clay on the kinetics of CH₄ hydrate-implication for energy recovery. *Chem. Eng. J.*, 437.
- Ren, J. J., Yin, Z. Y., Li, Q. P., Wu, F., Chen, D. Y., and Li, S. X. (2022b). Pore-Scale investigation of CH₄ hydrate kinetics in clayey-silty sediments by low-field NMR. *Energy and Fuels* 36 (24), 14874–14887. doi:10.1021/acs.energyfuels.2c03255
- Song, X. L., Nian, T. K., Mestdagh, T., and De Batist, M. (2023). Long- and short-term dynamic stability of submarine slopes undergoing hydrate dissociation. *Gas Sci. Eng.* 111, 204934. doi:10.1016/j.jgsce.2023.204934
- Sun, H. R., Chen, B. B., Pang, W. X., Song, Y. C., and Yang, M. J. (2022b). Investigation on plugging prediction of multiphase flow in natural gas hydrate sediment with different field scales. *Fuel* 325, 124936. doi:10.1016/j.fuel.2022.124936
- Sun, S. C., Gu, L. L., Yang, Z. D., Lin, H. F., and Zhang, C. X. (2023). Gas hydrate dissociation by depressurization along with ice occurrence and sand migration. *Gas Sci. Eng.* 109, 104853. doi:10.1016/j.jngse.2022.104853
- Sun, W. T., Wei, N., Zhao, J. Z., Kvamme, B., Zhou, S. W., Zhang, L. H., et al. (2022a). Imitating possible consequences of drilling through marine hydrate reservoir. *Energy* 239, 121802. doi:10.1016/j.energy.2021.121802
- Sun, Y. M., Li, S. D., Lu, C., Liu, S. M., Chen, W. C., and Li, X. (2021). The characteristics and its implications of hydraulic fracturing in hydrate-bearing clayey silt. *J. Nat. Gas Sci. Eng.* 95, 104189. doi:10.1016/j.jngse.2021.104189
- Tang, Q. Q., Chen, Y. B., Jia, R., Guo, W., Chen, W. Q., Li, X. S., et al. (2023). Effect of clay type and content on the mechanical properties of clayey silt hydrate sediments. *Geoenergy Sci. Eng.* 220, 111203. doi:10.1016/j.petrol.2022.111203
- Too, J. L., Cheng, A., Khoo, B. C., Palmer, A., and Linga, P. (2018a). Hydraulic fracturing in a penny-shaped crack. Part I: Methodology and testing of frozen sand. *J. Nat. Gas Sci. Eng.* 52, 609–618. doi:10.1016/j.jngse.2017.12.022
- Too, J. L., Cheng, A., Khoo, B. C., Palmer, A., and Linga, P. (2018b). Hydraulic fracturing in a penny-shaped crack. Part II: testing the crackability of methane hydrate-bearing sand. *J. Nat. Gas Sci. Eng.* 52, 619–628. doi:10.1016/j.jngse.2018.01.046
- Wan, Y., Wu, N., Hu, G., Xin, X., Jin, G., Liu, C., et al. (2018). Reservoir stability in the process of natural gas hydrate production by depressurization in the shenhu area of the south China sea. *Nat. Gas. Ind. B* 5 (6), 631–643. doi:10.1016/j.ngib.2018.11.012
- Wang, X. C., Sun, Y. H., Guo, W., Li, S. L., Chen, H. K., Peng, S. Y., et al. (2023b). 2D discrete element simulation on the marine natural gas hydrate reservoir stimulation by splitting grouting. *Gas Sci. Eng.* 110, 204861. doi:10.1016/j.jgsce.2022.204861
- Wang, X. C., Sun, Y. H., Li, B., Zhang, G. B. A., Guo, W., Li, S. L., et al. (2023a). Reservoir stimulation of marine natural gas hydrate—a review. *Energy* 263, 126120. doi:10.1016/j.energy.2022.126120
- Yang, D. H., Yan, R. T., Yan, M. Q., Lu, D., and Wei, C. F. (2023). Geomechanical properties of artificial methane hydrate-bearing fine-grained sediments. *Gas Sci. Eng.* 109, 104852. doi:10.1016/j.jngse.2022.104852
- Yin, Z. Y., Moridis, G., and Linga, P. (2019). On the importance of phase saturation heterogeneity in the analysis of laboratory studies of hydrate dissociation. *Appl. Energy* 255, 113861. doi:10.1016/j.apenergy.2019.113861
- Yu, Y. P., Liu, J. X., Li, B., and Sun, Y. H. (2022). Analysis of the hydraulic fracturing mechanism and fracture propagation law with a new extended finite element model for the silty hydrate reservoir in the South China Sea. *J. Nat. Gas Sci. Eng.* 101, 104535. doi:10.1016/j.jngse.2022.104535

- Zhan, L., Wang, Y., and Li, X. S. (2018). Experimental study on characteristics of methane hydrate formation and dissociation in porous medium with different particle sizes using depressurization. *Fuel* 230, 37–44. doi:10.1016/j.fuel.2018.05.008
- Zhang, W. D., Shi, X., Jiang, S., Cao, Q. Y., Wang, F., Wang, Z. Y., et al. (2020). Experimental study of hydraulic fracture initiation and propagation in highly saturated methane-hydrate-bearing sands. *J. Nat. Gas Sci. Eng.* 79, 103338. doi:10.1016/j.jngse.2020.103338
- Zhang, Z., Liu, L. L., Ning, F. L., Liu, Z. C., Sun, J. Y., Li, X. D., et al. (2022). Effect of stress on permeability of clay silty cores recovered from the Shenhu hydrate area of the South China Sea. *J. Nat. Gas Sci. Eng.* 99, 104421. doi:10.1016/j.jngse.2022.104421
- Zhao, Y. P., Kong, L., Liu, J. Q., Sang, S. K., Zeng, Z. Y., Wang, N., et al. (2023b). Permeability properties of natural gas hydrate-bearing sediments considering dynamic stress coupling: a comprehensive experimental investigation. *Energy*, 283.
- Zhao, Y. P., Liu, J. Q., Sang, S. K., Hua, L. K., Kong, L., Zeng, Z. Y., et al. (2023a). Experimental investigation on the permeability characteristics of methane hydrate-bearing clayey-silty sediments considering various factors. *Energy* 269, 126811. doi:10.1016/j.energy.2023.126811